Supporting Information

Qu *et al.* 10.1073/pnas.0805760105

SI Materials and Methods

Plant Materials. Mutant plants *dcl1–7*, *dcl2–1*, *dcl3–1*, *dcl4–2* have been described previously (1) and are kindly provided by Dr. James C. Carrington. Mutant *ago1–11* was a gift from Dr. Martienssen (2). Mutant *dcl1–9* was obtained from Dr. Olivier Voinnet's lab. Mutant *rdr6–11*, *drb4–1*, and *ago7–1* were ordered from Arabidopsis Biological Resource Center. All mutants were verified through genotyping and, except for *dcl1–7*, *dcl1–9*, and *ago1–11*, maintained as homozygous plants. For *dcl1–7*, *dcl1–9*, and *ago1–11*, seeds of heterozygous plants were maintained and homozygous plants were selected by their unique phenotypes. The plants were reared in growth chambers that are set at 20°C, 12-h daylight with a light intensity of 160–190 μmol/m^2/sec. The plants were infected at three weeks old for most mutants and 4–5 weeks old for *dcl1–7* and *ago1–11* mutants.

Viral Constructs. The TCV infectious clone and TCV-ΔCP (TCV-ΔNar) construct have been described previously (18). The TCV-GFP construct was made by first introducing an NcoI site into the CP coding region of the TCV infectious clone after the fifth amino acid residue. The modified TCV infectious clone was then digested with NcoI and MscI to remove the first half of the CP coding region, and to accommodate the GFP cDNA, which was PCR-amplified with primers that incorporate an *Nco*I site at its N terminus and an *Msc*I site at its C terminus, resulting in TCV-GFP. TCV-P19 was constructed by replacing GFP cDNA in TCV-GFP with TBSV P19. Replacement of GFP cDNA was a 555-bp fragment of *Arabidopsis* DCL1 cDNA (nucleotide position 867–1,422), with *Msc*I site at its 5′ end and *Nco*I site at its 3′ end, gave rise to TCV-DCL1. The creation of TCV-pG and TCV-irG has been described in Results and Discussions. Sequences of all oligo primers are available upon request.

To create the TCV-P19-GFP and TCV-P19-DCL1 constructs shown on Fig. S2, a 240-bp region of TCV CP cDNA immediately downstream of the P19 insert (between MscI site [nt position 3,387] and *Ehe*I site [nt position 3627]) was replaced with GFP or DCL1 cDNA fragments, both 298 bp long. Note that the DCL1 fragment used in TCV-P19-DCL1, which corresponds to nt position 1,912–2,210 of DCL1 cDNA, does not overlap with the DCL1 insert in TCV-DCL1 (nt position 867–1,422).

Plant Infection and RNA Analysis. For each mutant and the wildtype controls, at least six plants were infected with the infectious transcripts of clones described above, on three leaves per plant. The concentrations of inocula used were: wtTCV, 1 ng/μl; TCV-ΔCP and TCV-P19, 10 ng/μl; TCV-GFP, TCV-DCL1, TCV-pG, TCV-irG, TCV-P19-GFP, and TCV-P19-DCL1, 50 ng/μl. Approximately 20 μl of inoculum was applied per leaf.

At 4-dpi and 8-dpi, six inoculated leaves from six different plants infected with the same inoculum were pooled and total RNA was extracted. *U*ninoculated young leaves were collected for RNA extraction between 9–14 dpi. The RNA samples (5 μg each) were subjected to RNA blot hybridization with a probe that anneals to the 3′ untranslated region of TCV. Quantification of the gRNA was carried out by scanning the exposed X-ray films with a ChemiDoc XRS scanner (Bio-Rad, Hercules, CA) and generating the density readings of the gRNA bands with the help of QuantityOne 4.5.0 software (Bio-Rad). The relative levels were then determined by arbitrarily setting the value of TCV-ΔCP-infected samples as 1 and calculating the values of other samples accordingly.

For siRNA analysis, 5–15 μg total RNA was loaded onto a 0.1× TBE, 8 M urea, 16% polyacrylamide gel and run until the bromophenol blue dye migrated out. The separated RNAs were then transferred to a Nylon membrane and hybridized with ^{32}P-labeled oligonucleotides of desired sequences and polarities. The hybridization buffer was UltraHyb Oligo from Ambion, and the hybridization temperature was 40°C. After overnight hybridization, the membrane was washed three times, 20 min each, with 2× SSC, 0.5% SDS; at 50°C. For siRNA data shown in Fig. 2 and 4, the same set of membranes were stripped and sequentially hybridized with probes specific for (TCV+), (TCV-), (GFP+), and (GFP-) siRNAs.

SqRT-PCR. Total RNA samples were first treated with RNase-free DNase I provided by Ambion according to manufacturer's manual. One microgram of each RNA sample was then subjected to reverse transcription using SuperScript III (Invitrogen) reverse transcriptase, and respective reverse primers. The synthesized first strand cDNA was then subjected to PCR amplification with Lucigen's EconoTaq Plus Green 2X Master Mix.

1. Xie Z, *et al.* (2004) Genetic and functional diversification of small RNA pathways in plants. *PLoS Biol* 2:E104.

2. Haas G, *et al.* (2008) Nuclear import of CaMV P6 is required for infection and suppression of the RNA silencing factor DRB4. *EMBO J* , 10.1038/emboj.2008.129.

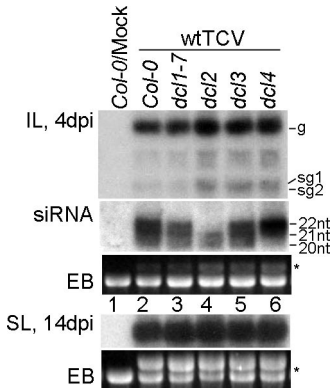

Fig. S1. RNA blot hybridizations showing accumulation levels of viral RNA and siRNAs of WT TCV (wtTCV) in four different *dcl* mutants. Note that wtTCV RNA accumulation is apparent even in EB-stained gel (* in *B*). The IL-specific siRNAs accumulated as three size classes in Col-0, *dcl1–7*, and *dcl3* plants, namely 22, 21, and 20 nt (lanes 2, 3, and 5 of the siRNA panel). The 22- and 21-nt siRNA levels were diminished in *dcl2* and *dcl4* plants, respectively (lanes 4 and 6). The 20-nt siRNAs were likely derived from 21-nt siRNAs, as they were also absent in *dcl4* mutants.

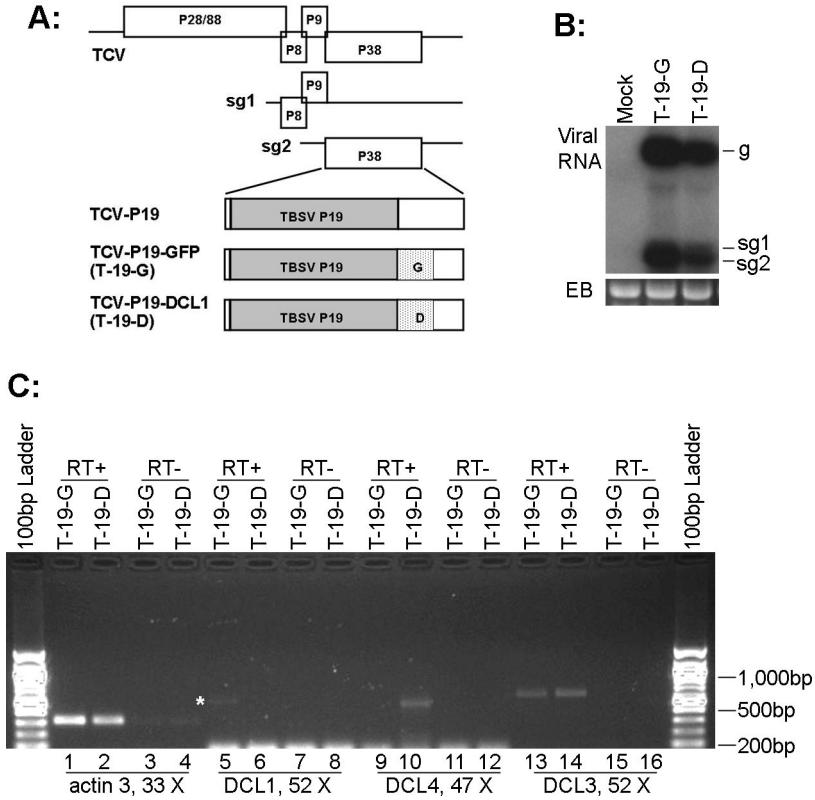

Fig. S2. VIGS down-regulation of DCL1 leads to up-regulation of DCL4 and DCL3. (*A*) The TCV-P19-GFP (T-19-G) and TCV-P19-DCL1 (T-19-D) constructs. (*B*) Northern blot hybridization showing that T-19-G and T-19-D replicate to easily detectable levels in inoculated leaves, with T-19-G RNA slightly more abundant. (*C*) Semi-quantitative RT-PCR showing that infection with T-19-D led to lower DCL1 mRNA level and higher DCL4 and DCL3 mRNA levels. A white star marks the faint DCL1 band present in the T-19-G-inoculated control leaves that is absent in T-19-D-inoculated leaves. Note that the numbers of cycles required to amplify DCL1 (52 X), DCL3 (52 X), and DCL4 (47X) are different.

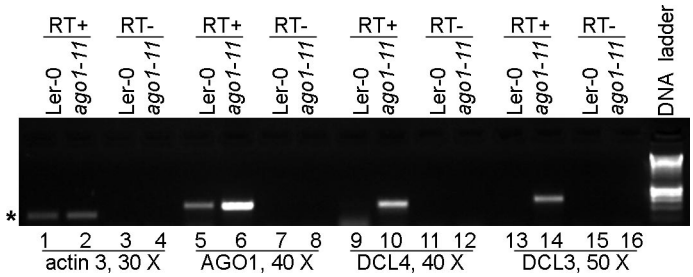

Fig. S3. SqRT-PCR analysis showing that both DCL4 and DCL3 are up-regulated in *ago1–11* leaves. The star (*) to the left of the image highlights the position of actin 3-specific PCR product.

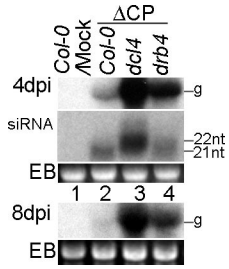

Fig. S4. RNA blot hybridization showing accumulation levels of TCV-ΔCP viral RNA and siRNAs in the inoculated leaves of *dcl4* and *drb4* mutant plants.

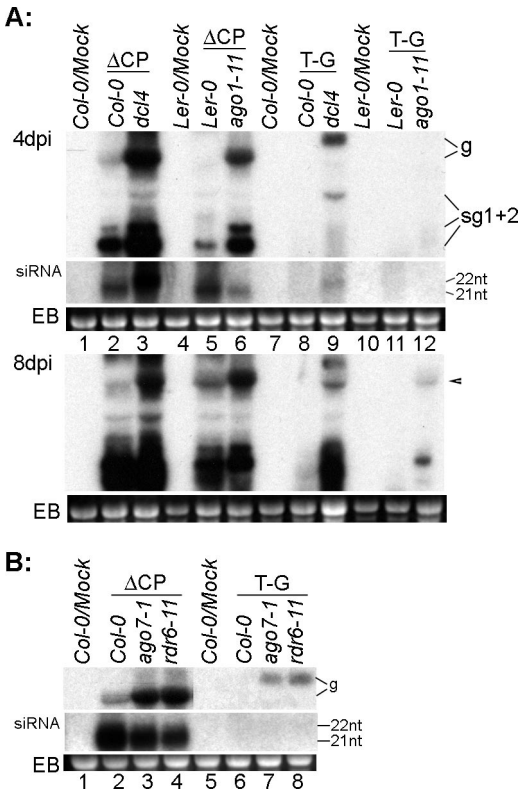

Fig. S5. Preferential targeting of viral RNAs by AGO1 and AGO7. (*A*) RNA blot hybridization showing side-by-side comparison of *dcl4* and *ago1–11* mutants infected with TCV-ΔCP and TCV-GFP (T-G). The top panel shows the viral RNA accumulation, whereas the middle panel shows the siRNA levels in the corresponding samples. (*B*) RNA blot hybridization showing the accumulation levels of TCV-ΔCP and TCV-GFP in *rdr6–11* and *ago7* plants.